Highly oriented photosynthetic reaction centres generate a proton gradient in synthetic protocells

Emiliano Altamura (a), Francesco Milano (b), Roberto R. Tangorra (a), Massimo Trotta (b), Omar Hassan Omar (c), Pasquale Stano (d) and Fabio Mavelli (a)

(a) Chemistry Department, University "Aldo Moro"; Via Orabona 4, I-70126 Bari, Italy. (b) CNR-IPCF, Istituto per i Processi Chimico Fisici, Via Orabona; 4, I-70126 Bari, Italy. (c) CNR-ICCOM, Istituto di Chimica dei Composti Organometallici; Via Orabona, 4, I-70126 Bari, Italy. (d) Science Department, Roma Tre University; Viale G. Marconi 446, I-00146 Rome, Italy.

Submitted to Proceedings of the National Academy of Sciences of the United States of America

Photosynthesis is responsible for the photochemical conversion of light into the chemical energy which fuels the planet Earth. The photochemical core of this process in all photosynthetic organisms is a transmembrane protein called the reaction center. In purple photosynthetic bacteria a simple version of this photo-enzyme catalyzes the reduction of a quinone molecule, accompanied by the uptake of two protons from the cytoplasm. This results in the establishment of a proton concentration gradient across the lipid membrane, which can be ultimately harnessed to synthesize ATP. Herein we show that synthetic protocells, based on giant lipid vesicles embedding an oriented population of reaction centers, are capable of generating a photo-induced proton gradient across the membrane. Under continuous illumination, the protocells generate a gradient of 0.061 pH units min^{-1}, equivalent to a proton motive force of 3.6 mV min^{-1}. Remarkably, the facile reconstitution of the photosynthetic reaction center in the artificial lipid membrane, obtained by the droplet transfer method, paves the way for the construction of novel and more functional protocells for synthetic biology.

photosynthetic reaction center | giant lipid lesicles | artificial cells | light transduction | proton gradient

Introduction

The synthesis of living cells from scratch is one of the most ambitious goals in biology and chemistry[1-6]. Initiated in the origin-of-life community[7-10], research on supramolecular assemblies modelling primitive cells has rapidly increased in the past few years. More recently the rapid expansion of synthetic biology[11] has given additional conceptual stimuli and technical tools to this field, especially by the so-called bottom-up approach[12]. Despite the recent progress, which is mainly focused on the reconstitution of essential biochemical functions inside confined environments[13] like phospholipid[4,5,14-19] and fatty acid vesicles[8,20,21], water-in-oil droplets[22], and coacervates[23], the primary generation of chemical energy by molecular machineries remains a missing key function.

In this paper, we try to fill this gap by constructing protocells capable of transducing light into chemical energy in the form of a pH gradient. To this aim, the photosynthetic reaction center (RC) extracted from *Rhodobacter sphaeroides* has been reconstituted in giant lipid vesicles. RC is a membrane-spanning protein located in biological membranes surrounded by other chlorophyll- based proteins (see SI Appendix, section S3a for a detailed description)[24,25] and it is the core of the photosynthetic apparatus of plants, algae and photosynthetic bacteria. However, if extracted from living systems and reconstituted in suitable lipid compartments, it can also work in the absence of its ancillary proteins. RC is composed of two highly hydrophobic subunits L and M, and the mostly hydrophilic H subunit[26]. These subunits cooperate, by a mechanism based on photon absorption[27], to catalyze the reduction of quinone species, removing protons from the cytoplasm (SI Appendix, Figs. S1-S2a,b). The RC photocycle (illustrated in SI Appendix, Fig. S2c) starts when RC absorbs a photon, and generates an electron-hole couple in the presence of an electron donor (reduced cytochrome c_2) and an electron acceptor (ubiquinone). While reduced cytochromes c_2 transfer electrons to RC from the external pool, protons are taken up from the cytoplasm by ubiquinone giving ubiquinol, thus establishing a pH gradient across the intra-cytoplasmic membrane. The proton gradient is used by the cell to fuel ATP synthesis[28] and ultimately the whole metabolism of the organism[29].

Previous works[30-40] have shown that RC can be reconstituted with the detergent depletion method[41] generally with random orientation in submicrometer liposomes[31,34-35,37-40]. However, partial (60%)[33] and high physiological orientation (90%)[30] have been also reported and it has been shown that experimental conditions play a decisive role in determining RC orientation[32,36,42]. RC reconstitution has been reported in random orientation in planar lipid bilayers[43-46] as well, even if high orientation can be also achieved in such systems[42]. We have already reported the generation of a transmembrane proton gradient in RC-containing conventional liposomes[40]. Herein we present a novel single-step procedure for reconstituting RC in giant lipid vesicles with high physiological orientation showing that the resulting RC@GUVs are able to convert light into a transmembrane pH gradient.

Results

Reconstitution of RC in GUVs membrane by means of the droplet transfer method. Giant unilamellar vesicles (GUVs)[47]

Significance

The photosynthetic reaction center (RC), an integral membrane protein at the core of bioenergetics of all autotrophs organisms, has been reconstituted in the membrane of giant unilamellar vesicles (RC@GUV) by retaining the physiological orientation at a very high percentage (90±1%). Owing to this uniform orientation, it has been possible to demonstrate that, under red-light illumination, photosynthetic RCs operate as nanoscopic machines which convert light energy into chemical energy, in the form of a proton gradient across the vesicle membrane. This result is of great relevance in the field of synthetic cell construction, proving that such systems can easily transduce light energy into chemical energy eventually exploitable for the synthesis of ATP.

Reserved for Publication Footnotes

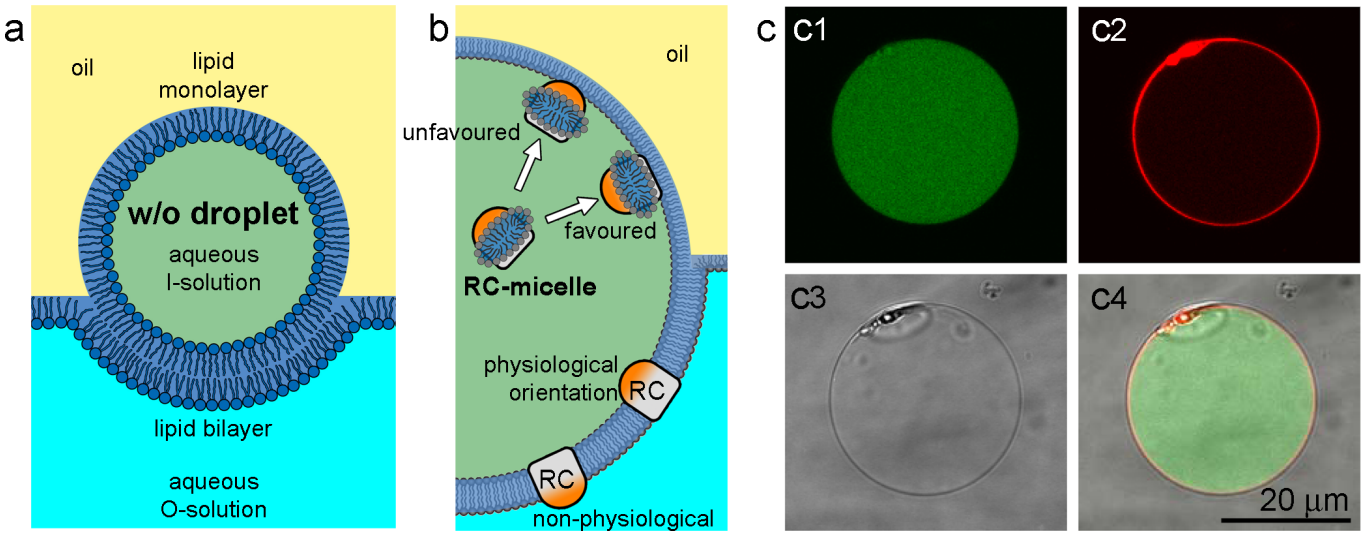

Fig. 1. Preparation of GUVs by the droplet transfer method[48]. (a) Water-in-oil (w/o) droplets, prepared by the emulsification of an aqueous solution (I-solution) in a lipid-rich oil phase, are transferred to an aqueous solution (O- solution) by centrifugation. **(b)** For preparing RC@GUVs, a detergent-stabilized RC solution (RC-micelles) is emulsified in oil, giving the w/o droplets. Owing to asymmetric RC-micelle structure a preferential "physiological" RC orientation is expected, namely, with the H subunit (in orange) facing toward the aqueous core of the droplets (the cytoplasm-like GUV lumen), and the photoactive dimer (SI Appendix, Fig. S2a,b) facing the GUV exteriors (in white). **(c)** RC@GUVs (POPC:POPG 9:1) as imaged by confocal microscopy. Red-fluorescent AE-RC was reconstituted in calcein-containing GUVs. **(c1)** Green fluorescence channel (calcein); **(c2)** red fluorescence channel (AE-RC); **(c3)** bright field; **(c4)** overlay of the c1, c2, and c3channels.

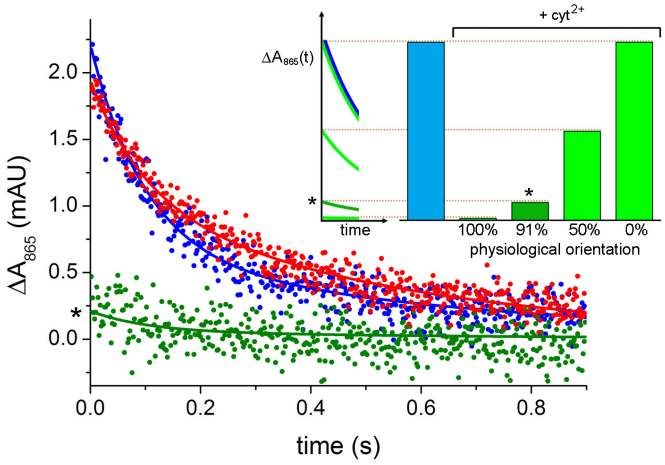

Fig. 2. Charge recombination of RCs reconstituted in giant vesicles after a saturating light flash. The points represent the experimental data, the lines are the bi-exponential best fit curves. Data refer to charge recombination in the absence (blue points) and in the presence (dark green points) of excess of reducing agent (cyt^{2+}). In a control experiment (red points), a full recovery of RC photo-activity is measured after the addition of an electron acceptor, the decylubiquinone (dQ) and the exhaustion of cyt^{2+}. Note that values in the y-axis represent the absolute values of $\triangle A_{865}$. In the inset, theoretical charge recombination curves in absence (blue) and in presence (green) of cyt^{2+}, corresponding to different RC orientation (100, 50, and 0 % of physiological orientation). The histogram represents the initial amplitude of the curves $\triangle A_{865}(0)$. Dark green bar, marked with the asterisk, refers to the experimental trace reported in the main plot.

were prepared using the droplet transfer method[48] (Fig. 1) since we envisaged that this method could be suitable for reconstituting transmembrane proteins with a high degree of physiological orientation. Purified RC from *R. sphaeroides* was first obtained by a well-established procedure requiring the detergent lauryldimethylamine *N*-oxide (LDAO) to extract the protein from the photosynthetic membrane and to solubilize it in aqueous solutions[49]. A homogeneous micellar solution was obtained

Table 1. Kinetic analysis of charge recombination experiments: bi-exponential decay fitting of experimental data reported in Fig. 2 (further details in SI section S3b).

sample	$\triangle A_0$ (mAU)	A_f (%)	A_s (%)	k_s (s^{-1})
RC@GUVs	2.21 ± 0.03	71 ± 3	29 ± 3	1.52 ± 0.09
RC@GUVs + cyt^{2+}	0.21 ± 0.01	71 ± 13	29 ± 13	1.50 ± 0.10
RC@GUVs + cyt^{2+} + dQ	1.94 ± 0.03	45 ± 2	55 ± 2	1.86 ± 0.06

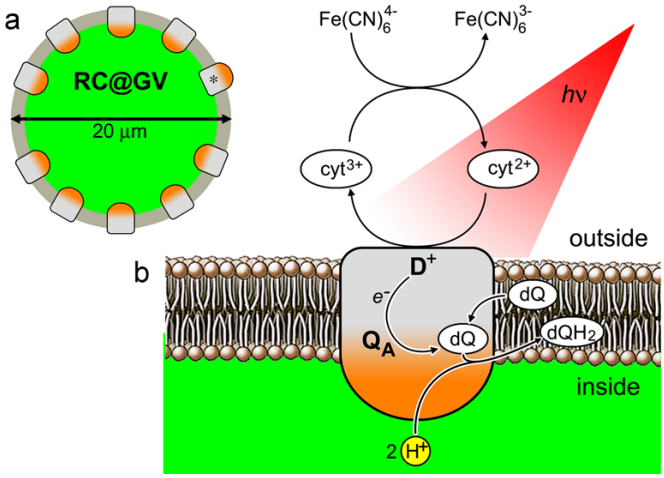

Fig. 3. Scheme of RC@GUVs function under red-light illumination. (a) RC is reconstituted, in highly oriented manner (90%) in the membrane of GUVs, whose average diameter is 20 µm. The asterisk marks a non physiologically oriented RC. **(b)** Detail of the photochemical mechanism generating the pH gradient.

with fully photo-active RCs surrounded by a toroid of LDAO molecules that shield the LM core from aqueous environment[50].

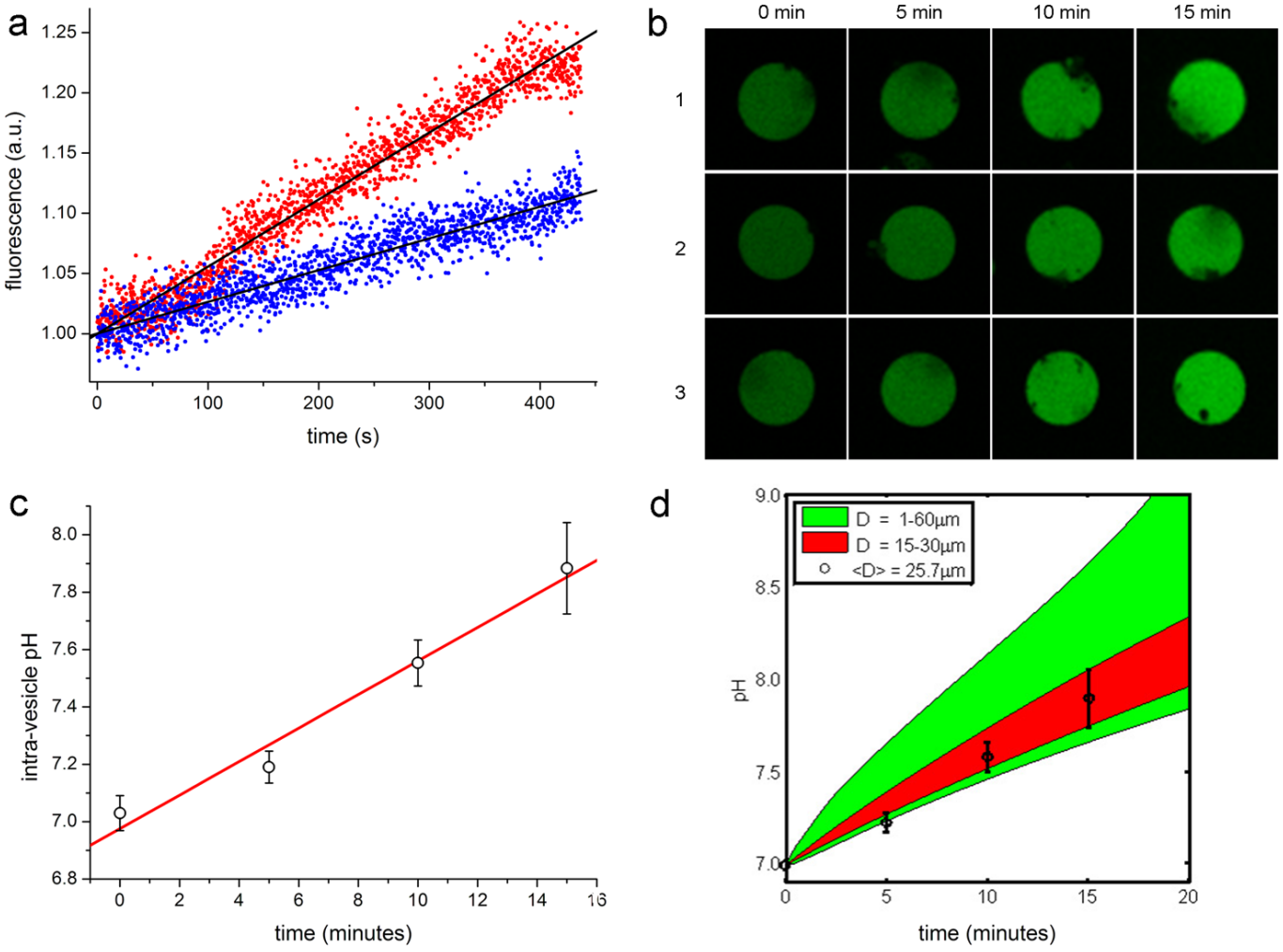

Fig. 4. Generation of a pH gradient by RC@GUVs. (a) Bulk fluorescence measurements of pyranine-containing RC@GUVs, which have been suspended in a fluorescence cuvette and illuminated from the top (SI Appendix, Fig. S9). Blue and red points refer to RC@GUVs with final RC concentration of 10 nM and 20 nM, respectively. Black lines represent the best fit straight-line , whose slopes are $(2.64 \pm 0.03)\times10^{-4}$ a.u. min^{-1} and $(5.57 \pm 0.03)\times10^{-4}$ a.u. min^{-1}, respectively, for the blue and red datasets. **(b)** Confocal images of three pyranine-containing RC@GUVs illuminated with red light. **(c)** Quantitative image analysis reveals the increase of intra-vesicle pH in time (fluorescence values converted by means of a calibration, see SI Appendix, section S2h). The best fit slope is 0.061 ± 0.004 pH units min^{-1}. **(d)** Comparison between the experimentally observed pH increase in the aqueous core of giant vesicles: circles with error bars (as in panel 4c) and the theoretical outcomes (colored bands).

To prepare RC@GUVs, the RC micelle solution was emulsified in mineral oil containing a mixture of phosphatidylcholine and phosphatidylglycerol (POPC:POPG 9:1). This emulsion was then layered on the aqueous solution generating a biphasic system and RC@GUVs were obtained after centrifugation (Fig. 1c).

Considering the RC reconstruction mechanism in vesicle membrane, it is reasonable to assume that, micelles when dispersed in w/o will deliver their protein cargo at the droplet w/o interface, mainly driven by hydrophobic interactions. Moreover, as RCs present asymmetric distribution of hydrophilic and hydrophobic regions, protein-containing micelles will have a preferential orientation while approaching to, and interacting with, the lipid monolayer of the w/o droplet, because the large hydrophilic H subunit prefers the aqueous phase (SI Appendix, Fig. S2a,b). It is expected that the chemical vectoriality of both RC-micelles and lipid monolayer will favor only one of the possible protein orientations in the w/o droplets before and during their transfer to the aqueous phase, so that a population of highly oriented RCs in the GUVs membrane should be obtained.

RC@GUVs prepared in such a way have an average diameter of 20±10 μm (statistical analysis performed on a population of 150 GUVs, Fig. S3) and are morphologically stable for at least two days when stored in the dark at room temperature. Quantitative image analysis shows calcein does not leak out from GUVs after 2 days from the preparation (SI Appendix, Fig. S4) proving also that traces of detergent, present as a consequence of the RC encapsulation, do not significantly affect the membrane stability.

The concentration of lipids and photoactive RCs, collected in 100 μL volume of the thus prepared GUVs suspension, were determined spectroscopically (SI Appendix, section S2g), resulting 440 μM and 0.2 μM, respectively, hence a protein/lipid molar ratio of 1/2200 was reached. RC@GUVs are characterized by a quite high RC density (~1200 RC molecules μm^{-2}), corresponding to roughly one third of the RC average density in the intracytoplasmic membranes of photosynthetic bacteria[51,52]. The collected GUVs were washed twice before further use, in order to remove any external fragments of RCs.

Fluorescently-labelled RCs were used to monitor the spatial distribution of the protein in GUVs. As a fluorophore, we selected a suitable fluorescent dye belonging to the aryleneethynylenes class, since these molecules emit[53] light efficiently and can be easily functionalized to be covalently conjugated to

biomolecules (SI Appendix, section S2a). In this work, we used the **7**-AE fluorophore (AE) (SI Appendix, Fig. S6)[54] that absorbs light at 445 nm and emits it in the red region at 602nm (SI Appendix, Fig. S7). The AE is covalently linked through an amide bond to the protein lysine residues by exploiting the succinimidyl ester derivative AE-NHS as an activated compound toward the reaction with amine groups in the lysines (Figure S8)[54]. The AE-RC conjugate can be easily visualized by confocal microscopy, allowing its localization in AE-RC@GUVs. Figure 2c shows images obtained by confocal laser scanning microscopy where vesicles display an uniform red fluorescent ring overlapping with the vesicle membrane, demonstrating a homogeneous incorporation of RC in the lipid bilayer of all GUVs.

RC is active and highly oriented. The photoactivity of reconstituted RC can be assessed by inducing the formation of an electron-hole couple by a short light flash and monitoring the time of the charge recombination reaction by following the absorbance at 865 nm (detailed mechanism reported in SI Appendix, section S3b). Fig. 2 shows the time decay of the charge-separated state induced by light flash: blue dots are the recovery of the dimer signal from the excited state after a saturating flash in RCs reconstituted in giant vesicles. From the initial absorbance: $^{\triangle}A865(0)$ = 2.21 ± 0.03 milli absorbance (mAU), the actual RC amount in the RC@GUVs preparation can be determined which corresponds to ~10% of the protein initially loaded in the w/o droplets. The bi-exponential fitting of the recorded trace (blue line) reveals that the fast charge-recombination from $D^+Q_A^{-\bullet}$ (A_f) accounts for about 71% of the overall signal, while the slow recombination from $D^+Q_AQ_B^{-\bullet}$ (A_s) contributes in a minor way (29%), showing that under these experimental conditions the QB-site is only occupied partially (Table 1, first row). The orientation of the RCs population in GUV membrane can be assessed by using the water soluble cytochrome c_2[30], the physiological electron-donor to the photo-oxidized dimer. In fact, both the reduced (cyt^{2+}) and the oxidized (cyt^{3+}) forms of the cytochrome are unable to cross the membrane. Therefore, the reduced cyt^{2+} added in excess externally to pre-formed RC@GUVs reacts only with the oxidized dimers exposed to the outer solution. The electron donation from the reduced cytochrome to the oxidized dimer: $D^+ + cyt^{2+} \rightarrow D + cyt^{3+}$ occurs very fast in the μs time scale preventing the charge recombination reaction. The dimers reduced by the cyt^{2+} will not contribute to the absorbance recorded at 865 nm. On an average, if the RCs reconstituted in the GUVs dispose across the lipid bilayer in random orientation, only half of the dimers faces toward the bulk solution. Under this condition, a saturating flash of light will generate the full population of D^+, but the signal will appear halved since the dimers oriented toward the bulk are re-reduced on a very fast time scale by cyt^{2+}. The other extreme possibilities, *i.e.* fully oriented RCs with the dimer facing the GUVs core, or fully oriented with the dimer facing the external aqueous solution, will give the full signal $^{\triangle}A_{865}(0)$ in presence of cyt^{2+} or the complete absence of signal respectively (Fig. 2, inset). The actual ratio of the D^+ absorbance change in the presence ($^{\triangle}A_{865}(0)_{cyt}$) and in the absence ($^{\triangle}A_{865}(0)$) of cyt^{2+} gives the fraction of RCs oriented in the bilayer with the dimer exposed to the outer solution. Hence, fully oriented RCs will have the ratio $^{\triangle}A_{865}(0)_{cyt}/^{\triangle}A_{865}(0)$ value equal to 0 when all RCs are oriented with the dimer outwards. The ratio assumes value 1 when all RCs are oriented with the dimer facing the GUVs water core. All other intermediate possibilities will have a ratio value ranging from 0 to 1.

Figure 2 (green points) shows the recovery of D in RC@GUVs in the presence of externally added cyt^{2+}. A small signal $^{\triangle}A_{865}(0)_{cyt}$ 0.21 ± 0.01 mAU is recorded, accounting for 9.5±0.6% of the $^{\triangle}A_{865}(0)$ value recorded in the absence of cyt^{2+} (Table 1, second row). This clearly indicates that the vast majority of photoactive proteins in RC@GUVs prepared by the droplet transfer method, 90±1%, are uniformly oriented and expose the dimer to the outer aqueous phase. Notably, this result also demonstrates that the large majority of vesicles prepared by the droplet transfer method are unilamellar, as reported elsewhere[55]. In fact, if RC was embedded in any internal lipid structure, as the internal membranes of multi-lamellar vesicles, it would not react with cyt^{2+} and therefore it would count as oppositely oriented.

As a further experimental test to check RC functionality, a suitable amount of decylubiquinone (dQ) was then added in order to oxidize all cyt^{2+} molecules, as a result of the RC photocycle (SI Appendix, Fig. S2c). In fact, dQ is an ubiquinone analogous that binds to the RC QB-site and accepts electrons as well[56]. When added to RC@GUVs suspension, it is expected that dQ will insert into the lipid membrane, diffuses and binds to RC QB-site. RC@GUVs were illuminated with repeated light pulses until the exhaustion of cyt^{2+}, which is converted to cyt^{3+} while dQ is reduced to decylhydroubiquinone dQH_2. Thus, having removed all the exogenous electron donors, the charge recombination signal reappeared. As shown in Fig. 2 (red points) and Table 1 (third row), the measured $^{\triangle}A_0$ value, in the presence of dQ (1.94 ± 0.03 mAU), is close to the original 2.21 ± 0.03 mAU value, demonstrating unequivocally the biochemical activity and the high orientation of RCs in GUVs. As expected, the slow pathway for charge recombination (k_s = 1.86 ± 0.06 s^{-1}) now becomes more relevant (55%), due to the presence of dQ in the QB-site.

RC converts light energy into a pH gradient across the GUVs membrane. The spontaneously achieved high-orientation of RCs in the bilayer of the GUVs having roughly 90% of the dimer facing the aqueous bulk and, consequently, ~90% of the QB-site facing the vesicle lumen, can be exploited to efficiently build a light-driven pH gradient across the GUVs membrane. Under continuous actinic illumination, and thanks to the electron-hole couple formation, the electrons will flow from the external donor (cyt^{2+}) to the acceptor (dQ in the QB-site) that will uptake protons from the vesicle aqueous core to form the quinol dQH2. Ultimately, this compounds accumulates in the bilayer. The net result of the photocycle is an intravesicle alkalinization that can be revealed using the pH-sensitive probe pyranine. Pyranine-containing RC@GUVs, prepared with low buffer capacity, were hence added with excess of dQ, a small amount of cyt^{2+}, and an excess of ferrocyanide acting as secondary electron donor. Under continuous irradiation, the pathway shown in Fig. 3 is established. The net stoichiometry of the main process is the oxidation of two ferrocyanide to ferricyanide, and the reduction of dQ to dQH_2,

$$2Fe(CN)_6^{4-} + dQ + 2H^+ \xrightarrow{2h\nu} 2Fe(CN)_6^{3-} + dQH_2$$

removing two protons per dQ molecule from the vesicle lumen.

Continuous red-light irradiation of pyranine-containing RC@GUVs (SI Appendix, Fig. S9) generated an increase of pyranine fluorescence over the whole vesicle population, shown in Fig. 4a for two different RC concentrations in the final suspension: 10 and 20 nM respectively. As can be seen, by doubling the RC concentration in the preparation, this amplifies the pH rate by a factor of 2.11±0.02.

The incipient proton gradient across the membrane of individual RC@GUVs was visualized by directly illuminating the vesicles in a microscopy slide well and imaging them with confocal microscopy. Figure 4b reports a series of fluorescence micrographs referring to pyranine-containing RC@GUVs at increasing irradiation time. Pyranine fluorescence increases over time as expected and the fluorescence intensity obtained by image analysis was converted to pH units via a calibration curve (SI Appendix, Fig. S10). The internal pH linearly increases in time, as shown in Fig. 4c, with a slope of 0.061 pH unit min-1, equivalent to one pH

unit in 16.4 min. The average rate of pH increase was converted in the rate of translocated proton per RC by a physico-chemical model that takes into account the GUV size, the RC density, and chemical composition of the vesicle lumen. According to some simplifying assumptions (detailed in SI Appendix, sections S5c,e) the observed pH increase corresponds to a calculated RC turnover rate of about 1.0 ± 0.1 protons min^{-1} per protein, equivalent to 2.5 × 10^6 protons min^{-1} per GUV. This value is our best estimate of RC function in GUVs in current experimental conditions and corresponds about 10% of the maximal RC turnover rate calculated from the photon flux density delivered to the microscope well (SI Appendix, section S5e). Moreover, it contributes for a proton motive force of ca. 3.6 mV min^{-1} ($\triangle$pH min^{-1} × 59mV). In order to test the robustness of the RC@GUV, the same sample was irradiated in a fluorimetric cuvette for 30min immediately after the preparation and later on 24h (stored in the dark at room temperature) by showing a comparable increase in the fluorescence of the encapsulated pyranine (SI Appendix, Fig. S11). These experiments show that GUVs retain the encapsulated pyranine and, at the same time, that the RC activity is largely (ca 80%) maintained (see SI Appendix, section S3c).

Moreover, based on the developed kinetic model (SI Appendix, section S5b), a statistical estimation of the pH change over time in the entire GUVs population was obtained taking into account the vesicle polydispersity in size and in RC content. As the GUV size distribution is experimentally known (SI Appendix, Fig. S13), by assuming a random distribution for the RC surface concentration, it is possible to derive the bivariate density function $P_{Ves}(D, C_{RC})$ that estimates the probability $P_{Ves}(D, C_{RC})\ dD\ dCRC$ to find a GUV with diameter in the $[D, D+dD[$ range and RC concentration in the $[C_{RC}, C_{RC}+dC_{RC}[$ interval (SI Appendix, Fig. S14). According to this model, the calculated displacements of the pH time course, weighted by the density probability $P_{Ves}(D, C_{RC})$ for the whole vesicle population, are reported as green band (1-60 µm) in Fig. 4d. The shown large diversity in GUV performances depends much more on the vesicles size dispersion than on the random distribution of the RC proteins in the lipid membrane. In fact the red band, that refers to vesicles with a restricted size range (15-30 µm), exhibits a more uniform behavior (Fig. 4b and Fig S16) which is much closer to those of the GUVs monitored experimentally. The comparison with the experimental data is good enough to validate the theoretical approach, although a statistical analysis on a larger vesicle population would be necessary. Since the number of RCs per GUV scales with the vesicle surface, whereas the variations of the proton concentration scales with the GUV volume, the model predicts small RC@GUVs generate a pH gradient faster than large ones (SI Appendix, Fig S15). It is also possible to estimate theoretically the behavior of the smaller RC@GUVs with diameters <12.5 µm range that represent the 27% of the entire population and remove intra-vesicle protons from 2 to 4 times faster than the average (SI Appendix, Fig. S15), resulting in a theoretical pH increase rate up to 0.106 pH units min^{-1}. This suggests that RC@GUV with optimized size in the range between 10-15µm would perform more efficiently and uniformly than those shown in this first report. Microfluidics fabrication could be used to produce almost completely monodispersed vesicle samples.

Conclusions

By employing the droplet transfer method, we have shown here the construction of an artificial cell model, based on bacterial RC, capable of transducing light into chemical energy. The reconstitution of RCs in the GUV membrane results in a uniform orientation (90±1%) with the dimer of the photo- enzyme facing the outer aqueous solution. This orientation reproduces the disposition of the proteins in the natural photosynthetic membrane allowing the establishment of a light induced pH change as in photosynthetic bacteria in this bio-mimetic system. Furthermore, these synthetic protocells show an RC surface density comparable to the in *vivo* intra-cytoplasmic membranes[52]. The measured proton translocation rate, 1.0 ± 0.1 protons min^{-1} per RC, generates chemical energy in the form of a pH gradient that can be eventually converted in chemical work. However, more in-depth analyses are required in order to investigate how vesicle size, membrane lipid compositions, trace amounts of residual detergent can affect the RC reconstitution, the RC@GUVs yield, the membrane permeability and the RC photoactivity, paving the way to future optimisations.

Accordingly to the presented methodology, other membrane proteins could be reconstituted in GUVs[57], *i.e.* ATP-synthase, which would transduce the RC-generated proton gradient to ATP synthesis. A preliminary analysis suggests that the topological features of ATP-synthase would allow its reconstitution in the desired orientation in RC-containing lipid vesicles, so that ATP can be produced within the GUVs lumen. This sharply contrasts with the usual reconstitution procedures of photosynthetic protein complexes[58-60] or artificial photosynthetic systems[61] where ATP is produced outside the vesicles. The presented study represents a step forward in the aim of assembling artificial cells capable of autonomously generating chemical energy.

Methods

Purification of reaction centre. Photosynthetic reaction centre (RC) was purified from the *a*- protobacterium *R. sphaeroides* (R-26 strain) according to a reported protocol[49], obtaining an aqueous solution of RC micelles stabilized by lauryldimethylamine *N*-oxide (LDAO) (0.03% w/v =1.3 mM) in 20 mM Tris-HCl (pH 8.0), 1 mM EDTA. RC-AE conjugate was prepared, in the same buffer, but in the presence of Triton X-100 (0.03% w/v = 0.48 mM) as described in SI Appendix, section S2b.

Preparation of giant vesicles. RC reconstitution in giant unilamellar vesicles (GUVs) was carried out by droplet transfer method39, which consists in transforming micrometre-sized lipid-stabilized water-in-oil (w/o) droplets in GUVs. The method employs the following three solutions: (*a*) the organic phase, consisting in 0.5 mM POPC/POPG 9/1 mol/mol dissolved in mineral oil; (*b*) the inner solution (I-solution), consisting in a freshly prepared RC-containing mixture (10 µM RC or AE-RC; 0.003% detergent; 5 mM Tris-HCl buffer pH 7.4 or 10µM Tris-HCl buffer pH~7.0; 200 mM sucrose); (*c*) the outer solution (O-solution) consisting in a freshly prepared 5 mM Tris-HCl buffer pH 7.4 or 10 µM Tris-HCl buffer pH~7.0, 200 mM glucose. GUVs are collected after 10 min centrifugation at 2500 rpm at room temperature (more details in SI Appendix, section S2d) and washed twice before being used. Note that the overall LDAO:lipid molar ratio is 1:170.

Charge recombination experiments. The RC@GUVs sample was diluted 1:8 with O-solution and placed in a 1 cm squared quartz fluorescence cuvette. GUVs were irradiated by xenon lamp flashes (~100 µs) placed orthogonal with respect to the measuring beam. The absorbance decay at 865 nm ($\triangle$A865), which mirrors the charge recombination in RC, was followed in time (for about 2 s). Data were collected onto a digital oscilloscope (Tektronics TDS-3200), and multiple traces (n = 64, delay time 2 s) were averaged to reach a sufficiently high signal-to-noise ratio. The concentration of the photoactive protein was estimated using $\Delta\varepsilon_{865}$ = 112,000 M^{-1} cm^{-1} (Ref. S4 in S.I.)

Orientation assay. Reduced cytochrome c_2 (cyt^{2+}, 5 µM) – freshly prepared by reduction of cyt^{3+} with ascorbate and purified by gel filtration chromatography on Sephadex G-25 – was added to RC@GUVs, and charge recombination was measured as indicated above. The fraction of oriented RC is obtained by comparing the initial amplitude of the charge recombination absorbance decay recorded in the presence $\Delta A_{865}(0)_{cyt}$ and in the absence $\Delta A_{865}(0)$ of cytochrome. Control experiments are described in SI Appendix, section S3e.

Generation of proton gradient in RC@GUVs. Pyranine-containing RC@GUVs were prepared by including 10 µM pyranine in a modified I-solution (10 µM Tris-HCl, pH 7.0 and 200 mM sucrose). Potassium ferrocyanide (10 mM), cyt^{3+} (5 µM), and decylubiquinone dQ (60 µM) were added to vesicles in order to allow the establishment of the photocycle (Fig. 3), Continuous light illumination was accomplished with a Schott KL 1500 illuminator equipped with a 150 W lamp by using an optical light guide (1 inch in diameter) for irradiating of the sample. Experiments were carried out by reading the increase of pyranine green fluorescence (*i*) as collective GUVs signal (by using a spectrofluorimeter), or (*ii*) as individual GUVs (by using a confocal microscope), further details in SI Appendix, section S2i.

Acknowledgements.

The authors acknowledge financial support from MIUR (PRIN n. 2010BJ23 MN *Nanostructured Soft Matter*) and (PONa300369, *Laboratorio*

Sistema), and from Apulia Region (Project cod. 31 "PHOEBUS"). Collaboration among the authors has been fostered by the European COST Actions CM1304 (*Emergence and Evolution of Complex Chemical Systems*) and TD1102 (*Phototech: Photosynthetic proteins for technological applications: biosensors and biochips*)

1. Pohorille A, Deamer D (2002) Artificial cells: prospects for biotechnology. *Trends Biotechnol*. 20:123–128.
2. Noireaux V, Libchaber A (2004) A vesicle bioreactor as a step toward an artificial cell assembly. *Proc Natl Acad Sci USA* 101:17669–17674.
3. Kurihara K, Tamura M, Shohda K , Toyota T Suzuki K , Sugawara T (2011) Self-reproduction of supramolecular giant vesicles combined with the amplification of encapsulated DNA. *Nat Chem* 3:775–781.
4. Kuruma Y, Stano P, Ueda T, Luisi P L (2009) A synthetic biology approach to the construction of membrane proteins in semi-synthetic minimal cells. *Biochim Biophys Acta* 1788:567–574.
5. Lentini R, Santero S P, Chizzolini F, Cecchi D, Fontana J, Marchioretto M, Del Bianco C, Terrell J L, Spencer A C, Martini L, Forlin M, Assfalg M, Dalla Serra M, Bentley W E, Mansy S S (2014) Integrating artificial with natural cells to translate chemical messages that direct E. coli behaviour. *Nat Commun* 5:4012.
6. Fujii S, Matsuura T, Sunami T, Nishikawa T, Kazuta Y, Yomo T (2014) Liposome display for in vitro selection and evolution of membrane proteins. *Nat Protoc* 9:1578–1591.
7. Morowitz H J, Heinz B, Deamer D W (1988) The chemical logic of a minimum protocell. *Orig Life Evol Biosph* 18:281–287.
8. Oberholzer T, Wick R, Luisi P L, Biebricher C K (1995) Enzymatic RNA replication in self-reproducing vesicles: an approach to a minimal cell. *Biochem Biophys Res Commun* 207:250–257.
9. Szostak J W, Bartel D P, Luisi P L (2001) Synthesizing life. *Nature* **409**:387–390.
10. Mansy S S, Szostak J W (2009) Reconstructing the emergence of cellular life through the synthesis of model protocells. *Cold Spring Harb Symp Quant Biol* 74:47–54.
11. de Lorenzo V, Danchin A (2008) Synthetic biology: discovering new worlds and new words. *EMBO Rep* 9:822–827.
12. Luisi P L, Ferri F,Stano P (2006) Approaches to semi-synthetic minimal cells: a review. *Naturwissenschaften* 93:1–13.
13. Küchler A, Yoshimoto M, Luginbühl S, Mavelli F, Walde P, (2016) Enzymatic reactions in confined environments, *Nat. Nanotech.* **11**:409-420.
14. Kita H, Matsuura T, Sunami T, Hosoda K, Ichihashi N, Tsukada K, Urabe I, Yomo T (2008) Replication of genetic information with self-encoded replicase in liposomes. *Chembiochem* 9:2403–2410.
15. Gardner P M, Winzer K, Davis B G (2009) Sugar synthesis in a protocellular model leads to a cell signalling response in bacteria, *Nat. Chem.* 1:377–383.
16. Stano P, Carrara P, Kuruma Y, Souza T P, Luisi P L (2011) Compartmentalized reactions as a case of soft-matter biotechnology: synthesis of proteins and nucleic acids inside lipid vesicles. *J Mater Chem* 21:18887–18902.
17. Nourian Z, Roelofsen W, Danelon C (2012) Triggered gene expression in fed-vesicle microreactors with a multifunctional membrane. *Angew Chem Int Ed Engl* 51:3114–3118.
18. Matsubayashi, H., Kuruma, Y. & Ueda, T. In vitro synthesis of the E. coli Sec translocon from DNA. Angew. Chem. Int. Ed. Engl. 53, 7535–7538 (2014).
19. Grotzky A, Altamura E, Adamcik J, Carrara P, Stano P, Mavelli F, Nauser T, Mezzenga R, Schluter A D, Walde P, (2012) Structure and Enzymatic Properties of Molecular Dendronized Polymer−Enzyme Conjugates and Their Entrapment inside Giant Vesicles . *Langmuir* 29:10831-10840.
20. Chen I A, Salehi-Ashtiani K, Szostak J W (2005) RNA catalysis in model protocell vesicles, *J Am Chem Soc* **127**:13213–13219.
21. Mansy S S, Schrum J P, Krishnamurthy M, Tobe S, Treco D A, Szostak J W (2008) Template-directed synthesis of a genetic polymer in a model protocell, *Nature* 454:122–125.
22. Kato A, Yanagisawa M, Sato Y T, Fujiwara K, Yoshikawa K (2012) Cell-Sized confinement in microspheres accelerates the reaction of gene expression. *Sci Rep* **2**:283.
23. Dora Tang T-Y, van Swaay D, deMello A, Ross Anderson J L, Mann S (2015) In vitro gene expression within membrane-free coacervate protocells. *Chem Commun (Camb)* 51:11429–11432.
24. Bahatyrova S, Frese R N, Siebert CA, Olsen J D, van der Werf K O, van Grondelle R, Niederman R A, Bullough PA, Otto C, Hunter CN (2004) The native architecture of a photosynthetic membrane. *Nature* **430:**1058-1062.
25. Niederman R A (2016) Development and dynamics of the photosynthetic apparatus in purple phototrophic bacteria. *Biochimica et Biophysica Acta* **1857**:232-246.
26. Allen J P, Feher G, Yeates T O, Komiya H, Rees D C, (1988) Structure of the reaction center from Rhodobacter sphaeroides R-26: protein-cofactor (quinones and Fe2+) interactions. *Proc Natl Acad Sci USA* 85:8487–8491.
27. Stowell M H, McPhillips T M, Rees D C, Soltis S M, Abresch E, Feher G (1997) Light-induced structural changes in photosynthetic reaction center: implications for mechanism of electron-proton transfer, *Science* **276**:812-816.
28. Junge W, Nelson N (2015) ATP Synthase *Annu Rev Biochem* **84**:631–57.
29. Allen J P, Williams J C (1998) Photosynthetic reaction centers. *FEBS Lett,* 438:5–9.
30. Pachence J M, Dutton L, Blasie J K (1979) Structural Studies On Reconstituted Reaction Center-Phosphatidylcholine Membranes. *Biochimica et Biophysica Acta,* 548:348-373
31. Overfield R E, Wraight C A (1980) Oxidation of cytochromes *c* and *c*2 by bacterial photosynthetic reaction centers in phospholipid vesicles. 1. Studies with neutral membranes. *Biochemistry* 19:3322–3327.
32. Hellingwerf K J (1987) Reaction centers from Rhodopseudomonas sphaeroides in reconstituted phospholipid vesicles. I. Structural studies. *J Bioenerg Biomembr* 19:203–223.
33. Venturoli G, Melandri A, Gabellini N, Oesterhelt D (1990) Kinetics of photosynthetic electron transfer in artificial vesicles reconstituted with purified complexes from Rhodobacter capsulatus. *Eur. J. Biochem*. 189:105-112
34. Baciou L, Rivas E, Sebban P (1990) $P^+Q_A^-$ and $P^+Q_B^-$ charge recombinations in *Rhodopseudomonas viridis* chromatophores and in reaction centers reconstituted in phosphatidylcholine liposomes. Existence of two conformational states of the reaction centers and effects of pH and o-phenanthroline, *Biochemistry* **29**:2966–2976.
35. Agostiano A, Catucci L, Colafemmina G, Della Monica M, Palazzo G, Giustini M, Mallardi A (1995) Charge recombination of photosynthetic reaction centers in different membrane models. *Gazz Chim Ital* 125:615-622.
36. Hara M, Ueno T, Fujii T, Yang Q, Asada Y, Miyake J Orientation of photosynthetic reaction center reconstituted in neutral and charged liposomes. *Biosci. Biotech. Biochem.* (1997) 61:1577-1579.
37. Palazzo G, Mallardi A, Giustini M, Berti D, Venturoli G (2000) Cumulant analysis of charge recombination kinetics in bacterial reaction centers reconstituted into lipid vesicles, *Biophys J* 79:1171–1179.
38. Trotta M, Milano F, Nagy L, Agostiano A (2002) Response of membrane protein to the environment: the case of photosynthetic Reaction Centre. *Materials Science and Engineering: C* 22:263–267.
39. Nagy L, Milano F, Dorogi M, Trotta M, Laczkó G, Szebényi K, Váró Gy, Agostiano A, Maróti P (2004) Protein/lipid interaction in the bacterial photosynthetic reaction center: phosphatidylcholine and phosphatidylglycerol modify the free energy levels of the quinones. *Biochemistry* 43:12913–12923.
40. Milano F, Trotta M, Dorogi M, Fischer B, Giotta L., Agostiano A, Maróti P, Kálmán L, Nagy L (2012) Light induced transmembrane proton gradient in artificial lipid vesicles reconstituted with photosynthetic reaction centers. *J Bioenerg Biomembr* (2012) 44:373–384.
41. Ollivon M, Lesieur S, Grabielle-Madelmont C, Paternostre M (2000) Vesicle reconstitution from lipid-detergent mixed micelles. *Biochim Biophys Acta* 1508:34–50.
42. Salafsky J, Groves J T, Boxer S G, Architecture and Function of Membrane Proteins in Planar Supported Bilayers: A Study with Photosynthetic Reaction Centers (1996) *Biochemistry* 35:14773-14781
43. Schönfeld M, Montal M, Feher G, (1979) Functional reconstitution of photosynthetic reaction centers in planar lipid bilayers. *Proc. Nati. Acad. Sci. USA* 76:6351-6355.
44. Packham N J, Packham C, Mueller P, Tiede P D, Dutton P L, (1980) Reconstitution DE Photochemically Active Reaction Centers In Planar Phospholipid Membranes. *Febs Letters* 110:101-106.
45. Gopher A, Blatt T Y, Schonfeld M, Okamura M Y, Feher G, Montal M, (1985) The effect of an applied electric field on the charge recombination kinetics in reaction centers reconstituted in planar lipid bilayers. *Biophys. J.* 48:311-320.
46. Wang L, Roth J S, Han X J, Evans S D (2015) Photosynthetic Proteins in Supported Lipid Bilayers: Towards a Biokleptic Approach for Energy Capture. *Small* 11:3306–3318
47. Walde P, Cosentino K, Engel H, Stano P (2010) Giant vesicles: preparations and applications. *Chembiochem* **11**:848–865.
48. Pautot S, Frisken B J, Weitz D A (2003) Engineering asymmetric vesicles. *Proc Natl Acad Sci USA* **100** 10718–10721.
49. Okamura M Y, Steiner L A, Feher G (1974) Characterization of reaction centers from photosynthetic bacteria. I. Subunit structure of the protein mediating the primary photochemistry in Rhodopseudomonas spheroides R-26. *Biochemistry* 13:1394–1403.
50. Roth M, Lewitt-Bentley M, Michel H, Deisenhofer J, Huber R, Oesterhelt D (1989) Detergent structure in crystals of a bacterial photosynthetic reaction centre. *Nature* 340:659–662.
51. Sener M K, Olsen J D, Hunter C N, Schulten K (2007) Atomic-level structural and functional model of a bacterial photosynthetic membrane vesicle. *Proc Natl Acad Sci USA* 104:15723–15728.
52. Geyer T, Mol X, Blass S, Helms V (2010) Bridging the gap: linking molecular simulations and systemic descriptions of cellular compartments, *PLOS ONE* 5:e14070.
53. Hassan Omar O, la Gatta S, Tangorra, R R, Milano F, Ragni R, Operamolla A, Argazzi R, Chiorboli C, Agostiano A, Trotta M, Farinola G M (2016) Synthetic antenna functioning as light harvester in the whole visible region for enhanced hybrid photosynthetic reaction centers. Bioconjugate Chem, 27(7): 1614–1623.
54. Milano F, Tangorra R R, Hassan Omar O, Ragni R, Operamolla A, Agostiano A, Farinola G M, Trotta M (2012) Enhancing the light harvesting capability of a photosynthetic reaction center by a tailored molecular fluorophore. *Angew Chem Int Ed Engl* 51:11019–11023.
55. Chiba M, Miyazaki M, Ishiwata S (2014) Quantitative Analysis of the Lamellarity of Giant Liposomes Prepared by the Inverted Emulsion Method. *Biophys J* 107:346–354.
56. Gopta O A, Semenov A Y, Bloch D A (2001) Electrogenic proton transfer in *Rhodobacter sphaeroides* reaction centers: effect of coenzyme Q10 substitution by decylubiquinone in the QB binding site. *FEBS Letters* 499:116–120.
57. Yanagisawa M, Iwamoto M, Kato A, Yoshikawa K, Oiki S (2011) Oriented Reconstitution of a Membrane Protein in a Giant Unilamellar Vesicle: Experimental Verification with the Potassium Channel KcsA. *J Am Chem Soc* 133:11774–11779.
58. Luo T J M, Soong R, Lan E, Dunn B, Montemagno C (2005) Photo-induced proton gradients and ATP biosynthesis produced by vesicles encapsulated in a silica matrix. *Nat Mater* 4:220–224.
59. Dezi M, Cicco A D, Bassereau P, Lévy D (2013) Detergent-mediated incorporation of transmembrane proteins in giant unilamellar vesicles with controlled physiological contents, *Proc Natl Acad Sci USA* **110**:7276–7281.
60. Feng X, Jia Y, Cai P, Fei J, Li J (2016) Coassembly of Photosystem II and ATPase as Artificial Chloroplast for Light-Driven ATP Synthesis, *ACS Nano* **10**:556–561.

61. Steinberg-Yfrach G, Liddell P A, Hung S, Moore A L, Gust D, Moore T A (1997) Conversion of light energy to proton potential in liposomes by artificial photosynthetic reaction centres. *Nature* 385:239-241